

Rare-earth doped LaF₃ nanocrystals for upconversion fluorescence

Guang-Shun YI^a and Gan-Moog CHOW^{a,b}

^a Molecular Engineering of Biological and Chemical Systems, Singapore-Massachusetts Institute of Technology, National University of Singapore, Singapore 119260, Republic of Singapore. E-mail: smaygs@nus.edu.sg

^b Department of Materials Science & Engineering, National University of Singapore, Singapore 119260, Republic of Singapore. Fax: 65 6874 3604; Tel: 65 6874 3325; E-mail: msecgm@nus.edu.sg

Abstract—Upconversion fluorescent nanocrystals, Yb-Er, Yb-Ho and Yb-Tm co-doped LaF₃ were chemically synthesized. The average particle size was 4.4 nm with a narrow size distribution of ± 0.3 nm. Under the 980 nm NIR excitation, the green, red and blue emission bands from these nanocrystals were observed, respectively. These nanocrystals have potential applications as bio-probes and displays.

Index Terms—fluorescence, LaF₃, nanocrystals, synthesis, upconversion

I. INTRODUCTION

Semiconductor nanocrystals (quantum dots, QDs) may be employed as bio-probes for analytical and biophysical applications. [1-4] They have the potential to replace the currently used fluorescent organic dyes as a new generation of sensitive bio-probes. Both QDs and fluorescent organic dyes are down-conversion fluorescent bio-probes, which emit one lower energy fluorescent photon after absorbing another higher energy UV or visible photon. The main problem of these probes in bio-applications is the autofluorescence (noise) from the analytes under UV and visible light. It decreases the signal-to-noise ratio, thus limiting the sensitivity.

The use of infrared-to-visible upconversion phosphors as bio-probes, which is able to absorb and combine two or more near-infrared (NIR) photons with lower energy to produce a higher energy photon in the visible spectrum, is a promising approach to address the issue of autofluorescence. This concept was first proposed by Zarling *et al.* [5,6] Compared with organic dyes, fluorescent proteins and quantum dots, the key advantages of upconversion phosphors are improved signal-to-noise ratio, increased tissue penetration, reduced photo-bleaching and reduced

photo-toxicity. [7,8]

Fabrication of upconversion fluorescent inorganic nanoparticles suitable as bio-probe remains as a major challenge. The size of targeted molecules (for example, proteins, oligonucleotides and other biomolecules in cells or tissues) range from several to tens of nanometers. An optimal bio-probe therefore should be small in size (≤ 10 nm) with a narrow size distribution. It should yield high fluorescent efficiency and should be water re-dispersible. [4]

To date, the most efficient infrared-to-visible upconversion phosphors are Yb-Er or Yb-Tm co-doped fluorides such as NaYF₄, YF₃, LaF₃, GdF₃ and oxysulphide like Y₂O₂S, [9] where fluorides and oxysulphide are the hosts, ytterbium (Yb) as the sensitizer (absorber) and erbium (Er) or thulium (Tm) as fluorescent center (emitter). Under the 980 nm NIR excitation, they produce different colors of visible upconversion fluorescence, depending on doping ions. These commercially available phosphors are however in bulk form that are usually prepared by high-temperature solid-state reactions. Converting these bulk phosphors into nanoparticles that satisfy the bio-probe criteria mentioned above remains difficult. To date, the 400 nm Yb-Er and Yb-Tm co-doped Y₂O₂S upconversion fluorescent particles had been synthesized. [10,11] These particles were too large for application as bio-probes. Smaller particles have also been made. [11] Other work focused on the synthesis of doped NaYF₄ nanoparticles. Yet these particles suffered from low efficiency. [12,13]

Here we overview our recent work on the synthesis and properties of (Yb-Er)-, (Yb-Ho)- and (Yb-Tm)- doped LaF₃ nanocrystals. [14] These nanocrystals had an average size of 4.4 nm and a narrow size distribution (± 0.3 nm). They were easily dispersed in organic solutions and subsequently formed a clearly transparent colloidal solution. Green, red and blue emission bands were observed from these colloidal solutions, respectively, under the 980 nm irradiation.

II. EXPERIMENTAL

A. Chemicals

Lanthanum chloride heptahydrate ($\text{LaCl}_3 \cdot 7\text{H}_2\text{O}$, 99.99%), ytterbium chloride hexahydrate ($\text{YbCl}_3 \cdot 6\text{H}_2\text{O}$, 99.99%), erbium chloride hexahydrate ($\text{ErCl}_3 \cdot 6\text{H}_2\text{O}$, 99.99%), holmium chloride hexahydrate ($\text{HoCl}_3 \cdot 6\text{H}_2\text{O}$, 99.99%), thulium chloride hexahydrate ($\text{TmCl}_3 \cdot 6\text{H}_2\text{O}$, 99.99%), and sodium fluoride (NaF) were obtained from Sigma-Aldrich (Sigma-Aldrich, Singapore). Ammonium di-*n*-octadecyldithiophosphate was synthesized according to the literature.[15] Ultra pure water (18.0 M Ω) from a Milli-Q deionization unit was used throughout the experiment. Rare earth chloride stock solutions with a concentration of 0.4 mol.L⁻¹ were prepared by dissolving $\text{LaCl}_3 \cdot 7\text{H}_2\text{O}$, $\text{YbCl}_3 \cdot 6\text{H}_2\text{O}$, $\text{ErCl}_3 \cdot 6\text{H}_2\text{O}$, $\text{HoCl}_3 \cdot 6\text{H}_2\text{O}$ and $\text{TmCl}_3 \cdot 6\text{H}_2\text{O}$ respectively in de-ionized water. The final solutions were maintained at pH 2 to avoid hydrolysis.

B. Characterization

The nanocrystals were investigated using transmission electron microscopy (TEM) and x-ray diffraction (XRD). The upconversion fluorescence spectra were measured using a luminescence spectrometer with an external 980nm laser diode (2W, continuous wave) as the excitation source in place of the xenon lamp in the spectrometer. The spectrometer was operated at the bioluminescence mode, with gate time 100ms, delay time 0ms, cycle 0 and flash count 1. The sample was measured in two ways. For powder nanocrystals, 0.2 g sample was filled in the Powder holder and reproducibly positioned in the Front Surface accessory. For colloidal samples, a nanocrystal concentration of 0.1 wt.-% in dichloromethane was used.

C. Synthesis of the nanocrystals

In a typical procedure for the preparation of $\text{LaF}_3:12\%\text{Yb},3\%\text{Er}$ nanocrystals, 0.378g of NaF (9mmol) was dissolved in 50mL of de-ionized water. Then 50 ml of ethanol was added and the whole solution was heated to 70°C. 2.585 g (4mmol) ammonium di-*n*-octadecyldithiophosphate was subsequently added and dissolved. Another solution was prepared by mixing 8.5ml of 0.4mol.L⁻¹ LaCl_3 , 1.2ml of 0.4 mol.L⁻¹ YbCl_3 and 0.3ml of 0.4 mol.L⁻¹ ErCl_3 stock solutions together (4mmol rare earth ions totally) and swiftly injected into the NaF solution through a 10 ml syringe. White precipitates instantly appeared. After 2 h, the reaction mixture was placed in a 60°C oven for 2 h, an oil product layer was seen to segregate to the bottom of the mixture. The product was separated, and washed three times using anhydrous ethanol and once with de-ionized water. After drying for two days under vacuum, 0.6374g white powder was obtained.

For the synthesis of the other two nanocrystals, a molar ratio of La:Yb:Ho = 79:20:1 for $\text{LaF}_3:\text{Yb},\text{Ho}$, and La:Yb:Tm = 89:10:1 for $\text{LaF}_3:\text{Yb},\text{Tm}$, were adopted for the respective preparation following the same procedures.

III. RESULTS AND DISCUSSION

A. Morphology, structure and composition of the nanocrystals

Figure 1 shows the typical TEM bright field image of the $\text{LaF}_3:12\%\text{Yb},3\%\text{Er}$ nanocrystals. The dispersed particles suggested that the long chain ligand on the crystal surface prevented aggregation. The average diameter of the nanocrystals was 4.4 nm, with a standard derivation of ± 0.3 nm. Figure 1b is a high-resolution TEM image of $\text{LaF}_3:12\%\text{Yb},3\%\text{Er}$ nanocrystals. Most of the nanocrystals were equiaxed with well-defined crystallinity. Similar TEM results were also observed for $\text{LaF}_3:20\%\text{Yb},1\%\text{Ho}$ and $\text{LaF}_3:10\%\text{Yb},1\%\text{Tm}$ nanocrystals.

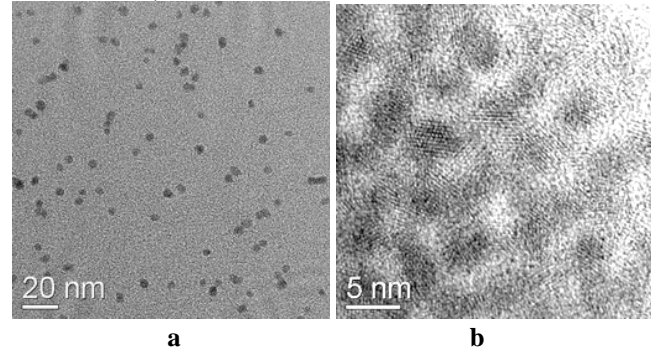


Fig. 1. (a) TEM micrograph of well-dispersed $\text{LaF}_3:12\%\text{Yb},3\%\text{Er}$ nanocrystals at a magnification of 100K. (b) TEM micrograph of $\text{LaF}_3:12\%\text{Yb},3\%\text{Er}$ nanocrystals at higher magnification of 600K. High crystallinity of the particles could be observed.

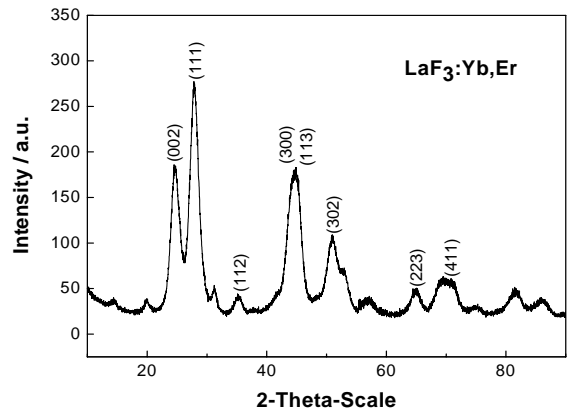


Fig. 2. X-ray powder diffraction patterns of the $\text{LaF}_3:12\%\text{Yb},3\%\text{Er}$ nanocrystals. Similar TEM results were also observed for $\text{LaF}_3:20\%\text{Yb},1\%\text{Ho}$ and $\text{LaF}_3:10\%\text{Yb},1\%\text{Tm}$ nanocrystals.

Figure 2 shows the XRD of the $\text{LaF}_3:12\%\text{Yb},3\%\text{Er}$ nanocrystals. Due to the small x-ray coherence domain size (small particle size), peak broadening was observed. The x-ray peak positions and intensities of the nanocrystals were similar and showed slight deviations from the hexagonal bulk LaF_3 crystal (PDF 72-1435). The average particle size estimated by line-broadening was 4.3 nm. Compared with

TEM results, the particles were confirmed to be single crystals. Similar XRD results were also obtained for $\text{LaF}_3\text{:}20\%\text{Yb},1\%\text{Ho}$ and $\text{LaF}_3\text{:}10\%\text{Yb},1\%\text{Tm}$ nanocrystals, respectively.

The ligand-capped $\text{LaF}_3\text{:}12\%\text{Yb},3\%\text{Er}$, $\text{LaF}_3\text{:}20\%\text{Yb},1\%\text{Ho}$ and $\text{LaF}_3\text{:}10\%\text{Yb},1\%\text{Tm}$ nanocrystals, were easily dispersed in organic solvents and formed a transparent colloidal solution. For organic solvents such as dichloromethane, chloroform and hexane, as high as 5 mg nanocrystals were dissolved in 1 ml of solvents. When an equal volume of ethanol was added in the organic solutions, their dispersion significantly increased. Since the ligand itself preferred to disperse in such ethanol-organic solutions, it enhanced the dispersibility of the nanocrystals in such systems.

B. Upconversion fluorescence

Figure 3 shows the room-temperature upconversion fluorescence spectra (Fig. 3 a, c and e) and their corresponding mechanisms (b, d and f) of $\text{LaF}_3\text{:}12\%\text{Yb},3\%\text{Er}$, $\text{LaF}_3\text{:}20\%\text{Yb},1\%\text{Ho}$ and $\text{LaF}_3\text{:}10\%\text{Yb},1\%\text{Tm}$ nanocrystals. For $\text{LaF}_3\text{:}12\%\text{Yb},3\%\text{Er}$ nanocrystals (Fig. 3a), under 980 nm NIR excitation, there were three emission peaks at 520.8, 545 and 658.8 nm, which were assigned to $^4\text{H}_{11/2}$ to $^4\text{I}_{15/2}$, $^4\text{S}_{3/2}$ to $^4\text{I}_{15/2}$ and $^4\text{F}_{9/2}$ to $^4\text{I}_{15/2}$ transition of erbium, respectively. [12,16,17] With the 980nm excitation, Yb^{3+} (sensitizer) absorbed one 980 nm photon and then transferred it to emitter Er^{3+} . The Er^{3+} received the energy and its ground-state ($^4\text{I}_{15/2}$) electron was excited to $^4\text{I}_{11/2}$ level. A second photon from Yb^{3+} promoted the electron to $^4\text{F}_{7/2}$ level. The excited electron decayed first non-radiatively to $^2\text{H}_{11/2}$, $^4\text{S}_{3/2}$ and $^4\text{F}_{9/2}$ levels. When it decayed further to the ground state, emission at 520.8, 545 and 658.8 nm occurred, as shows in Fig. 3b. For $\text{LaF}_3\text{:}20\%\text{Yb},1\%\text{Ho}$ nanocrystals, the strong red emissions at 644.73 and 657.8 nm (Fig. 3c) were assigned to the $^5\text{F}_5$ — $^5\text{I}_8$ transition, and the weaker green emission at 542.4 nm corresponded to $^5\text{S}_2$ — $^5\text{I}_8$ transition (Fig. 3d). [18-20] For $\text{LaF}_3\text{:}10\%\text{Yb},1\%\text{Tm}$ nanocrystals, the blue emission band at 475.2 nm corresponded to the transition from $^1\text{G}_4$ to $^3\text{H}_6$. A strong near infrared emission at 800.2 nm was attributed to the transition from $^1\text{G}_4$ to $^3\text{H}_5$ (Fig. 3, e and f). [21]

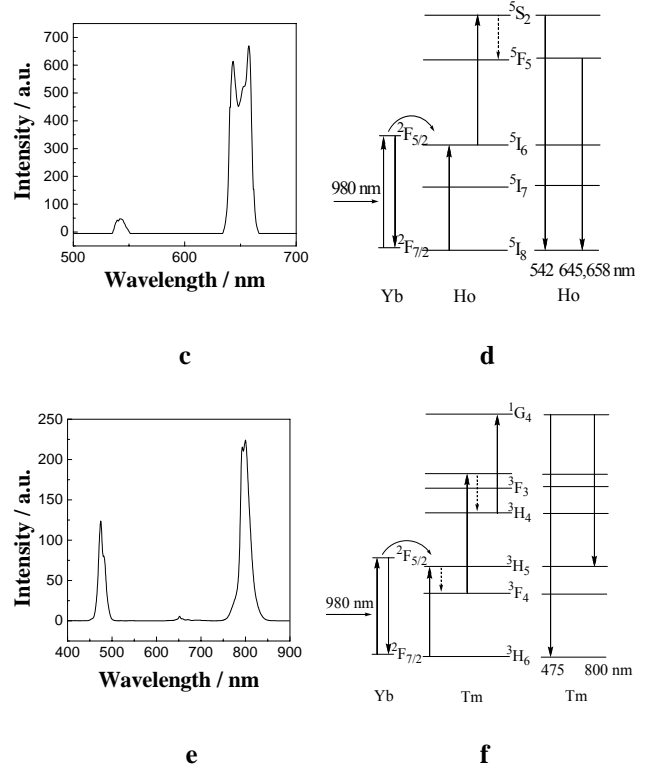
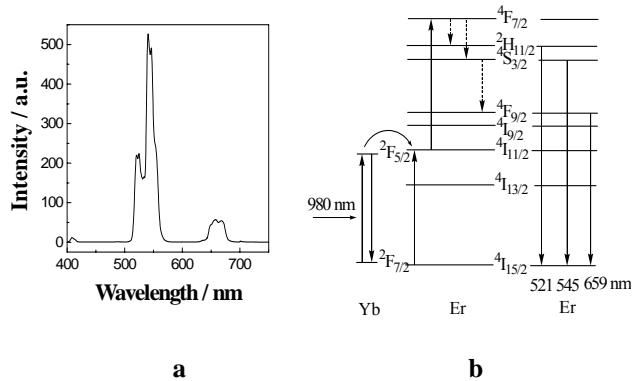


Fig. 3. Room-temperature upconversion fluorescence spectra (a, c and e) and corresponding mechanism (b, d and f) of the $\text{LaF}_3\text{:}12\%\text{Yb},3\%\text{Er}$, $\text{LaF}_3\text{:}20\%\text{Yb},1\%\text{Ho}$ and $\text{LaF}_3\text{:}10\%\text{Yb},1\%\text{Tm}$ nanocrystals under the 980 nm NIR excitation. Dotted arrows indicate nonradiative energy transfer and solid arrows refers to radiative processes.

From Figure 3, the three nanocrystals yielded different fluorescent emissions under the same 980 nm NIR excitation. For the three nanocrystals, the four strong peaks were: 475.2 nm blue emission from $\text{LaF}_3\text{:}10\%\text{Yb},1\%\text{Tm}$, 545 nm green emission from $\text{LaF}_3\text{:}12\%\text{Yb},3\%\text{Er}$, 657.8 nm red emission from $\text{LaF}_3\text{:}20\%\text{Yb},1\%\text{Ho}$ and 800.2 nm NIR emission for $\text{LaF}_3\text{:}10\%\text{Yb},1\%\text{Tm}$. These results indicated the promising potential of these materials as bio-probes, especially in the multiple labelling. Under the 980 nm NIR excitation, it is possible to simultaneously detect multiple analytes labeled with different colors of probes.

The measured upconversion fluorescent efficiency of the $\text{LaF}_3\text{:}12\%\text{Yb},3\%\text{Er}$ nanocrystals, was 5-times-higher than our previously reported cubic phase $\text{NaYF}_4\text{:}20\%\text{Yb}^{3+},2\%\text{Er}^{3+}$ nanocrystals.[12] However, it remains weaker (1-2 orders of decrease) when compared with their corresponding bulk phosphors from solid-state synthesis. Further work on size-surface effects on upconversion properties, surface functionalization and sensitivity of molecular detection are currently being pursued.

ACKNOWLEDGMENT

We thank B.H. Liu for help of HRTEM measurements. G.S. Yi was supported by a postdoctoral fellowship of the Singapore-Massachusetts Institute of Technology Alliance

(SMA). G.M. Chow thanks the support of NUS academic research funds and the grant of US office of Naval Research.

References

1. W. C. W. Chan and S. M. Nie, "Quantum dot bioconjugates for ultrasensitive nonisotopic detection," *Science* **281**, 2016-2018 (1998).
2. M. Bruchez, M. Moronne, P. Gin, S. Weiss, and A. P. Alivisatos, "Semiconductor nanocrystals as fluorescent biological labels," *Science* **281**, 2013-2016 (1998).
3. D. Gerion, F. Pinaud, S. C. Williams, W. J. Parak, D. Zanchet, S. Weiss, and A. P. Alivisatos, "Synthesis and properties of biocompatible water-soluble silica-coated CdSe/ZnS semiconductor quantum dots," *Journal of Physical Chemistry B* **105**, 8861-8871 (2001).
4. B. Dubertret, P. Skourides, D. J. Norris, V. Noireaux, A. H. Brivanlou, and A. Libchaber, "In vivo imaging of quantum dots encapsulated in phospholipid micelles," *Science* **298**, 1759-1762 (2002).
5. Zarling, D. A., Rossi, M. J., Peppers, N. A., Kane, J., Faris, G. W., Dyer, M. J., Ng, S. Y., and Schneider, L. V. Up-converting reporters for biological and other assays using laser excitation techniques. SRI, I. N. T. E. [US Patent 5674698].
6. F. van de Rijke, H. Zijlmans, S. Li, T. Vail, A. K. Raap, R. S. Niedbala, and H. J. Tanke, "Up-converting phosphor reporters for nucleic acid microarrays," *Nature Biotechnology* **19**, 273-276 (2001).
7. J. G. White, J. M. Squirrell, and K. W. Eliceiri, "Applying multiphoton imaging to the study of membrane dynamics in living cells," *Traffic* **2**, 775-780 (2001).
8. J. A. Feijo and N. Moreno, "Imaging plant cells by two-photon excitation," *Protoplasma* **223**, 1-32 (2004).
9. G. Blasse and B. C. Grabmaier, *Luminescent Materials*, (Springer, Berlin, 1994).
10. Sanjurjo, A., Lau, K.-H., Lowe, D., Canizales, A., Jijang, N., and Wong, V. production of substantially monodisperse phosphor particles. [US Patent 6039894]. 2000.
11. P. Corstjens, S. Li, M. Zuiderwijk, S. Adam, R. S. Niedbala, and H. Tanke, "infrared up-converting phosphors for bioassays," *IEEE Proc. -Nanobiotechnol.* **152**, 64-72 (2005).
12. G. S. Yi, H. C. Lu, S. Y. Zhao, G. Yue, W. J. Yang, D. P. Chen, and L. H. Guo, "Synthesis, characterization, and biological application of size-controlled nanocrystalline NaYF₄ : Yb,Er infrared-to-visible up-conversion phosphors," *Nano Letters* **4**, 2191-2196 (2004).
13. S. Heer, K. Kompe, H. U. Gudel, and M. Haase, "Highly efficient multicolour upconversion emission in transparent colloids of lanthanide-doped NaYF₄ nanocrystals," *Advanced Materials* **16**, 2102-+ (2004).
14. G. S. Yi and G. M. Chow, "Colloidal LaF₃:Yb,Er, LaF₃:Yb,Ho and LaF₃:Yb,Tm nanocrystals with multicolor upconversion fluorescence," *Journal of Materials Chemistry* **15**, 4460-4464 (2005).
15. J. W. Stouwdam and F. C. J. M. van Veggel, "Near-infrared emission of redispersible Er³⁺, Nd³⁺, and Ho³⁺ doped LaF₃ nanoparticles," *Nano Letters* **2**, 733-737 (2002).
16. S. L. Zhao, Y. B. Hou, and L. Sun, "Upconversion luminescence of ZBLAN:Er³⁺,Yb³⁺," *Journal of Northern Jiaotong University* **24**, 89-92 (2000).
17. G. S. Yi, B. Q. Sun, F. Z. Yang, D. P. Chen, Y. X. Zhou, and J. Cheng, "Synthesis and characterization of high-efficiency nanocrystal up-conversion phosphors: Ytterbium and erbium codoped lanthanum molybdate," *Chemistry of Materials* **14**, 2910-2914 (2002).
18. F. Lahoz, I. R. Martin, and D. Alonso, "Theoretical analysis of the photon avalanche dynamics in Ho³⁺-Yb³⁺ codoped systems under near-infrared excitation," *Physical Review B* **71**, (2005).
19. F. Lahoz, I. R. Martin, and A. Briones, "Infrared-laser induced photon avalanche upconversion in Ho³⁺-Yb³⁺ codoped fluorindate glasses," *Journal of Applied Physics* **95**, 2957-2962 (2004).
20. F. Z. Yang, G. S. Yi, D. P. Chen, and J. Cheng, "Synthesis and up-conversion luminescence properties of nanocrystal Yb, Ho co-doped sodium yttrium fluoride," *Chemical Journal of Chinese Universities-Chinese* **25**, 1589-1592 (2004).
21. S. Heer, O. Lehmann, M. Haase, and H. U. Gudel, "Blue, green, and red upconversion emission from lanthanide-doped LuPO₄ and YbPO₄ nanocrystals in a transparent colloidal solution," *Angewandte Chemie-International Edition* **42**, 3179-3182 (2003).